Tetrahedron 68 (2012) 8311–8317

Contents lists available at SciVerse ScienceDirect

Tetrahedron

journal homepage: www.elsevier.com/locate/tet

One catalyst for both enantiomers: uncovering the inversion of enantioselectivity in cinchona-mediated desymmetrization of glutaric *meso*-anhydrides

Trpimir Ivšić [a], Jurica Novak [b], Nađa Došlić [b], Zdenko Hameršak [a,*]

[a] Department of Organic Chemistry and Biochemistry, Rudjer Bošković Institute, PO Box 180, 10002 Zagreb, Croatia
[b] Department of Physical Chemistry, Rudjer Bošković Institute, PO Box 180, 10002 Zagreb, Croatia

ARTICLE INFO

Article history:
Received 13 April 2012
Received in revised form 13 June 2012
Accepted 10 July 2012
Available online 21 July 2012

Keywords:
Desymmetrization
Enantioselectivity
Density functional calculations
Asymmetric synthesis
Hydrogen bonding

ABSTRACT

A puzzling inversion of enantioselectivity dependent on catalyst loading was observed during the quinine-mediated desymmetrization of glutaric *meso*-anhydrides. This study presents the improvement of the catalytic path by the inclusion of carboxylic acid additives up to synthetically useful levels. The novel protocol utilizing 0.1 equiv of alkaloid and xanthene-9-carboxylic acid at room temperature (rt) was found comparable to the protocol requiring 1.1 equiv of alkaloid at −30 °C. Thus, by altering the protocol the same catalyst produces the opposite enantiomer.

This occurrence was rationalized by an extensive computational study of the interactions governing the molecular complexes formed by quinine, methanol, 3-methylglutaric anhydride, and the acetic acid. It was found that in a quinine catalyzed reaction the alcohol and the anhydride were directly hydrogen bonded to the catalyst. On the other hand, in the reaction with additive the acid intercalates between the alcohol and quinine. Due to this insertion the alcohol approaches the anhydride from the opposite face, in agreement with the observed inversion of enantioselectivity

1. Introduction

The enantioselective desymmetrization of cyclic *meso*-anhydrides[1] (Scheme 1) is of critical importance in the total syntheses of numerous biologically active substances,[2–5] including Pregabalin,[6] Biotin,[7] Baclofen,[8] etc. The asymmetric opening of cyclic *meso*-anhydrides was first put forward by Oda[9] and Aitken.[10] The stoichiometric protocol with natural cinchona alkaloids was further developed by Bolm and co-workers.[11] Alternatively, a catalytic amount of modified cinchona alkaloids including ethers,[12] ureas or thioureas,[13] and sulfonamides[14] was also found to steer the reaction toward the desired enantiomer. Modified cinchona alkaloids provide exceptionally high enantioselectivities with succinic anhydrides, but in the case of more demanding glutaric anhydrides inferior results are obtained with the same catalyst loading.[13] Thus, in the case of glutaric anhydrides, especially when larger quantities of products are needed, the use of easily available, inexpensive, and recoverable unmodified alkaloids is still the best option.

Recently reported was a Pregabalin synthesis[6a] where the quinine-mediated ring opening of 3-isobutylglutaric anhydride was the key step. At low catalyst loading an unexpected inversion of enantioselectivity has been observed.[15] More generally it has been

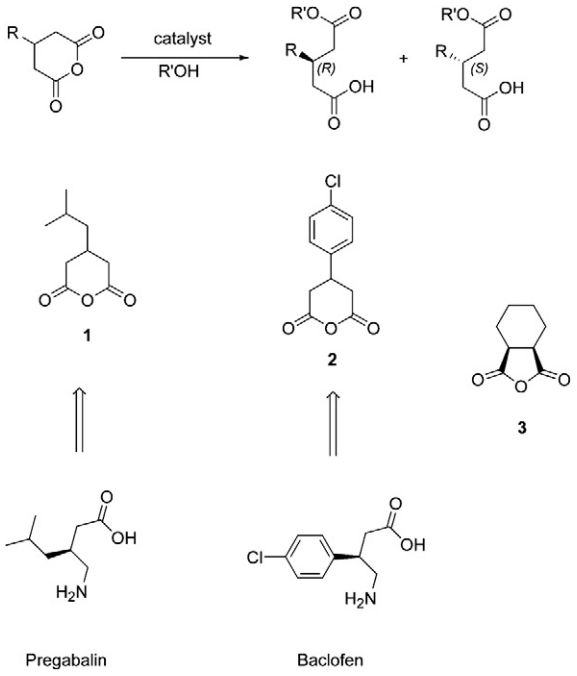

Scheme 1. Desymmetrization of glutaric *meso*-anhydrides.

* Corresponding author. Fax: +385 14680108; e-mail address: hamer@irb.hr (Z. Hameršak).

0040-4020/$ – see front matter © 2012 Elsevier Ltd. All rights reserved.
http://dx.doi.org/10.1016/j.tet.2012.07.035

demonstrated that organic acids as additives also invert the direction of enantioselectivity. Here we elaborate further on these findings and explore the synthetic utility of the alkaloid–acid co-catalyst approach as our first goal.

The mechanism of desymmetrization of *meso*-cyclic anhydrides by alcohol nucleophiles has been the subject of controversial discussions in the literature. In the nucleophilic catalysis,[10,16] the reaction is initiated by the attack of the amino group of the quinidine on the sterically less-hindered side of the anhydride resulting in the formation of a chiral acylammonium salt. The intermediate is stabilized via a hydrogen bond between the OH group of the catalyst and the carboxylate moiety. In the next step the alcohol reacts with the salt yielding the ester product. Alternatively in the general base catalysis proposed by Oda and co-workers[9] the alcohol is deprotonated by the amino group of the catalyst. In the subsequent step a nucleophilic attack of the resulting methoxide onto the anhydride leads to ring opening. Again, the formation of a hydrogen bond between the OH group of the catalyst and the carboxylate moiety facilitates the reaction. Recently, Dedeoglu and co-workers[17] shed light on the energetics of the two pathways. Based on the DFT calculations of a system consisting of a *meso*-cyclic anhydride and a model catalyst, (1*R*,2*R*)-2-(piperidin-1-yl)cyclohexanol, they have shown that the formation of the intermediate salt in the nucleophilic catalysis is energetically highly unfavorable. While the study undoubtedly points toward general base catalysis, the experimentally observed stereochemistry could not be explained on the basis of model calculations.[17]

Therefore, the second goal of this paper is to unravel the interactions in quinine-mediated ring opening of cyclic *meso*-anhydrides leading to the observed stereochemistry, as well as to elucidate the role of organic acids in the inversion of enantioselectivity. Specifically, we focus on the hydrogen bonding interactions and show that both, the original enantioselectivity and the inversed one can be traced back to the pro-chirality of the most abundant reaction complexes.

2. Results and discussion

We present first the experimental results on the inversion of enantioselectivity in alkaloid and alkaloid–acid catalyzed opening of glutaric anhydrides, and then explore the enantioselectivity of both reactions.

2.1. Synthetic potential

As mentioned in Introduction, we reported an inversion of enantioselectivity in the quinine catalyzed desymmetrization of glutaric anhydrides at low catalyst loading.[15] Specifically, in the case of anhydride **1** it was found that a catalyst loading of 160% produces about 40% ee of (*R*)-product, while a 10% loading yields 40% ee of (*S*)-product. In contrast, succinic anhydrides tend to produce racemic products if less of alkaloid is loaded (see Fig. 1).[10,11] Recently, Bolm also reported a similar reversion of enantioselectivity for alkaloid-mediated thiolyses of succinic *meso*-anhydrides.[18] The fact that at low catalyst loading a specific product–base complex inverts the direction of opening of glutaric anhydrides encouraged us to verify whether some other organic acid additives could improve the stereoselectivity. More than 25 different carboxylic acids were tested and a representative selection is compiled in Table 1.

The best enantioselectivities were achieved with acids possessing phenylacetic acid substructure (entries 3, 4 (X9C), and 8) as well as with 2-thiophene-acetic acid (entry 7), which can be considered as phenylacetic acid congener. We also noted that the direction of opening is no longer dependent on catalyst loading, and

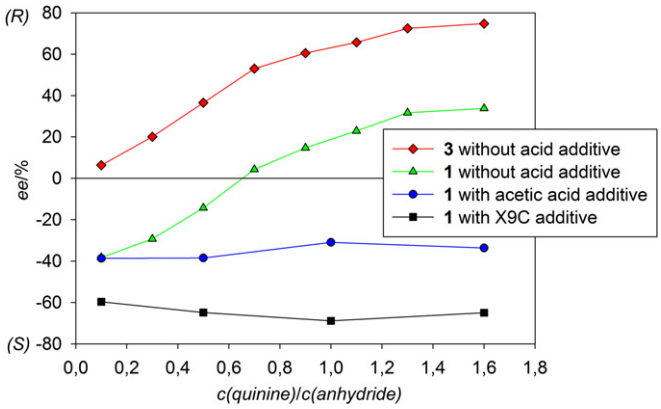

Fig. 1. Influence of catalyst loading on enantioselective opening of **1** and **3**. All reactions were performed in toluene (0.1 M with respect to anhydride) with 1.5 equiv of benzyl alcohol at rt. For reactions with acid additives, acid/quinine molar ratio was 2.

Table 1
Influence of acid additives on the desymmetrization of anhydride (**1**)

No.	Acid	ee[a]/%	No.	Acid	ee[a]/%
1	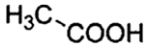	36	5	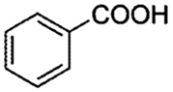	47
2	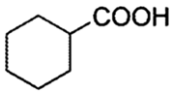	45	6	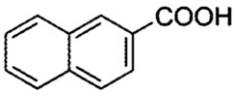	38
3	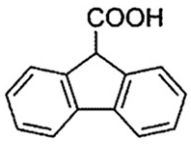	53	7	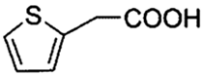	55
4	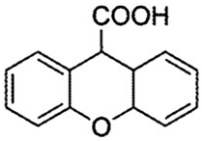	63	8	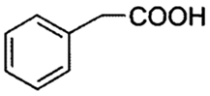	54

Reaction conditions: 0.1 M anhydride **1** in toluene, 0.5 equiv of quinine, 1 equiv of acid, 1.5 equiv of BnOH, rt.
[a] Major enantiomer (*S*)-configuration, determined by chiral HPLC on chiralcel AS (EtOH/hexane/TFA=2:98:0.1).

that better enantioselectivities are obtained with aprotic solvents (see Table 2).

On the other hand, as shown for urea and thiourea derived alkaloids, dilution effects the enantioselectivity.[13,19,20] Lowering the anhydride concentration from 0.125 to 0.025 M raises the enantioselectivity from 85% ee to 96% ee.[13] The same effect of dilution was observed with the quinine/acid combination (Fig. 2). Although high dilution improves the enantioselectivity, the reaction rate is significantly lowered—at 0.005 M solution the reaction was found incomplete after 6 days.

The enantioselecivity of the reaction can significantly be improved by lowering the reaction temperature when the alkaloid is employed in stoichiometric quantity. With the quinine/acid type of catalyst, lowering the temperature causes a minor improvement in the enantioselectivity, but a drastic reduction of the reaction rate. Finally, the influence of quinine/acid ratio on enantioselectivity was explored. For both acid additives the selectivity of the reaction reached its maximum at a base/acid ratio of 1:2 (Fig. 3).

Table 2
Solvent effect on opening selectivity

Entry	Solvent	ee/%	ee[a]/%
1	Chloroform	50.2	68
2	Toluene	47.5	65
3	*i*-Pr_2O	43.5	—
4	MTBE	39.6	—
5	Dioxane	26.5	—
6	THF	15	—

Reaction conditions: 0.1 M anhydride **1** solution, 0.5 equiv of quinine, 1 equiv of benzoic acid, 1.5 equiv of BnOH, 65 h at rt.
[a] Xanthene-9-carboxylic acid as additive.

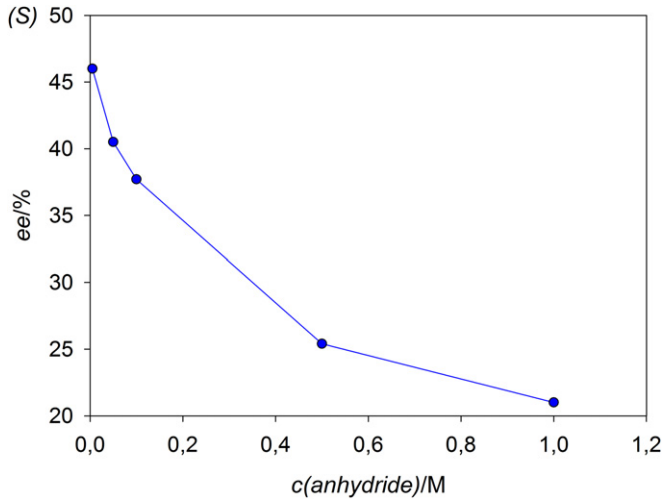

Fig. 2. Dilution effect on opening selectivity. Reaction conditions: anhydride **1** in toluene, 0.5 equiv quinine, 1 equiv acetic acid, 1.5 equiv BnOH, 65 h at rt.

To verify the synthetic utility of the enantioselective opening of 3-substituted glutaric *meso*-anhydrides catalyzed by the alkaloid–acid complexes, this methodology was compared with the stoichiometric approach (Scheme 2). Anhydrides **1** and **2** were chosen because their hemiester products provide an easy access to both enantiomers of pharmacologically interesting compounds (Pregabalin, Baclofen) in a multigram scale, while xanthene-9-carboxylic acid was found to be the most promising acid additive. The results are compiled in Table 3. With all anhydrides and all catalysts comparable results were obtained. Enantioselectivities were in the range of 56–73%, which is quite good bearing in mind that unmodified, easily available, and recyclable catalysts were used, and that glutaric anhydrides open with lower enantioselectivities in comparison with succinic. We should mention that the latter are typically used for catalytic activity testing.

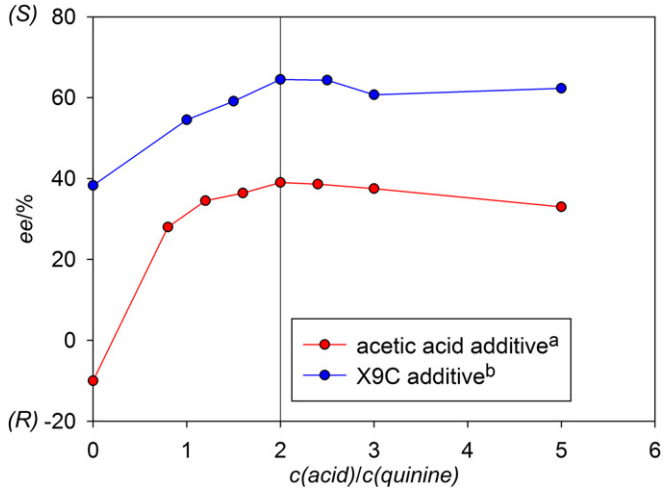

Fig. 3. Quinine/acid ratio effect on opening selectivity. [a]Reactions of anhydride **1** (6 mL of 0.1 M toluene solution) and 1.5 equiv BnOH with 0.5 equiv of quinine and acetic acid at rt. [b]Reactions of anhydride **1** (6 mL of 0.1 M toluene solution) and 1.5 equiv BnOH with 0.1 equiv of quinine and xanthene-9-carboxylic acid at rt.

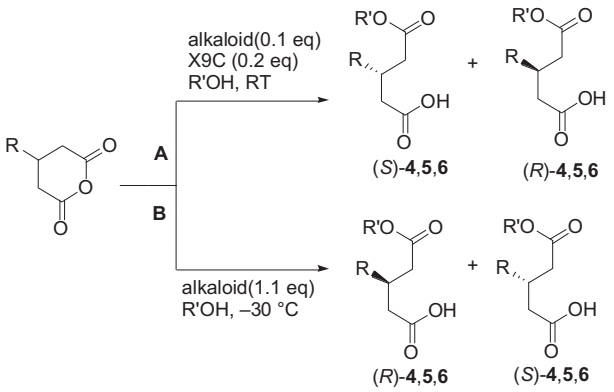

Scheme 2. Methodologies for enantioselective anhydride opening.

Table 3
Enantioselective opening of anhydrides **1** and **2**. Comparison of methodologies[a]

Anhydride	Method[b]	R′	*T*/°C	Time	η[d]/%	ee[e]/%	Product
1	A(0.1QD+X)	Bn	rt	22 h	70	73	(*R*)-**4**
1	B(1.1Q)	Bn	−25	23 h	72	64	(*R*)-**4**
1	A(0.1Q+X)	Bn	rt	18 h	n.i.[c]	65	(*S*)-**4**
1	A(0.1Q+X)	Cinn	rt	18 h	n.i.[c]	61	(*S*)-**5**
1	B(1.1Q)	Cinn	−25	25 h	85	69	(*R*)-**5**
2	A(0.1QD+X)	Bn	rt	2 d	82	72	(*R*)-**6**
2	B (1.1Q)	Bn	−35	7 d	60	77	(*R*)-**6**
2	A(0.1Q+X)	Bn	rt	2 d	87	56	(*S*)-**6**
2	B(1.1QD)	Bn	−35	7 d	74	62	(*S*)-**6**

[a] Reactions were carried out with 10 mmol of anhydrides, 0.1 M solution in toluene, 1.5 equiv of alcohol until >90% conversion was reached.
[b] Methods: (A) 0.1 equiv of quinidine (QD) or quinine (Q), 0.2 equiv of xanthene-9-carboxylic acid (X); (B) 1.1 equiv of quinine (Q) or quinidine (QD).
[c] Scale: 0.5 mmol.
[d] Isolated yield.
[e] Determined by chiral HPLC.

The slightly lower yields on isolated monoesters of anhydrides **1** and **2** compared to the conversion can be attributed to slow ester hydrolysis and the emulsification properties of their potassium salts during the work-up, which comprises successive washing of alkaline aqueous solution of monoester with organic solvent to remove residual alcohol.

Altogether the alkaloid–xanthene-9-carboxylic acid complex was found to have several advantages when compared with natural alkaloids in stoichiometric amount: lower catalyst loading, faster reaction, and the most important—an ambient reaction temperature.

2.2. Computational study

The conformational space of cinchona alkaloids has been intensively studied.[21,22] Several combined experimental and theoretical studies indicate that the open conformer of cinchona alkaloids, known as Open(3), is the most populated one at room temperature in apolar solvents.[22] In the following we focus on this conformer.

In principle, a series of plausible initial geometries of the three molecular complex consisting of quinine, methanol, and 3-methylglutaric anhydride required for full geometry optimizations at the B3LYP-D3/6-31G(d,p) level of theory can be obtained from classical molecular dynamics simulations. However, force field calculations are not adequate for describing the hydrogen bonding and dispersive interactions that determine the enantioselective ring opening, and the size of the system prevents the use of long DFT/ab initio molecular dynamics runs needed to explore the rather rough conformational landscape. Hence, our initial structures were based on a series of educated guesses facilitating both the nucleophilic and the general base catalysis. As the results of full geometry optimizations at the B3LYP/6-31 G(d) level we found nine distinct structures spanning an energy range of 13.97 kcal/mol. The four lowest structures plus another four obtained by inverting the stereochemical face of the anhydride have been reoptimized at the B3LYP-D3/6-31G(d,p) level. The relative energies, predicted stereochemistry of the final product, and selected geometrical parameters are compiled in Table 4.

Generally we have found that all investigated structures are stabilized by two hydrogen bonds, one between the alcohol and the quinuclidine amine, and the other one between the oxygen of one of the carboxyl groups and the quinine OH. The distance between the quinuclidine N and the closest carbonyl C atom of the anhydride is relatively large, in the range between 4.2 Å and 4.6 Å. In contrast, the distance between the methanol O and the closest carbonyl C atom is much shorter (2.7–3.2 Å). The geometries of these complexes point to the general base catalysis mechanism of desymmetrization of cyclic anhydrides.

Table 4
Relative energies, predicted chirality, and selected geometry parameters of the four lowest energy structures as obtained at the B3LYP-D3/6-31G(d,p) level of theory. The prediction of chirality is based on the ratio of the bond lengths *d*(C1–O6)/*d*(C5–O6). The numeration of atoms is given in Scheme 3

Conf.	E/kcal mol^{-1}	Predict. config.	Distance/Å			
			$d1/d2$[a]	(O,N)[b]	(O,O)[c]	(O,C)[d]
A	0.00	*R*	1.37/1.41	2.76	2.82	3.07
A′	1.47	*S*	1.41/1.36	2.75	2.84	2.69
B	0.12	*R*	1.37/1.41	2.76	2.83	3.02
B′	1.13	*S*	1.41/1.37	2.75	2.84	2.82

[a] Bond lengths ratio *d*(C1–O6)/*d*(C5–O6).
[b] H-bond distance between methanol O–H and quinuclidine N.
[c] H-bond distance between quinine OH and the closest carbonyl O.
[d] Distance between methanol O–H and the non H-bonded carbonyl C.

Fig. 4 displays the lowest energy structure (conformer **A**) and the corresponding chiral structure (conformer **A′**). The latter was obtained by reflecting the anhydride in the plane defined by the atoms C(1)–O(6)–C(5) and subsequent full geometry optimization (see Scheme 3). The energy difference between **A** (Fig. 4, top left) and **A′** conformers (Fig. 4, top right) is 1.47 kcal/mol, while the energy difference between conformer **B** and conformer **B′** is 1.01 kcal/mol.

Conformers **A** and **B** are stabilized by two hydrogen bonds, one between the alcohol and the quinuclidine N, and the other one between the pro-*S* carboxyl group and the catalyst OH. The natural bonding orbital (NBO) analysis reveals that there is virtually no difference in the charges between the two carbonyl C atoms. Because of the involvement of the pro-*S* carbonyl in the hydrogen bond with quinine OH, the pro-*R* carbonyl is more flexible and hence more prone to the methoxide nucleophilic attack.

Assuming the base catalyzed mechanism we predict in both cases a likely formation of the (*R*)-products. In an analogous way, the less stable conformers **A′** and **B′** feature a hydrogen bond between the quinine OH and the pro-*R* carboxyl group. This leads to the exposure of the pro-*S* carbonyl, elongation of the pro-*S* C–O bond and to the likely formation of the (*S*)-product. Comparing the geometries of the four conformers it is apparent that they are stabilized by a comparable network of hydrogen bonding interactions. A closer look at the geometries, however, reveals that the stabilization of the pro-*R* conformers with respect to the pro-*S* ones stems from more favorable steric interactions and in particular from the larger separation between methanol and the anhydride hydrogen atoms in the axial position. For example in **A** the distance between methanol O and the two axial atoms H_A and H_D is 2.41 Å and 2.51 Å, respectively, while a closer contact with H_E of 2.33 Å is found in **A′**.

The addition of organic acids causes the inversion of enantioselectivity. Preliminary exploration of the configurational space of the acetic acid, quinine, methanol, and 3-methylglutaric anhydride complex at the B3LYP/6-31G(d) level of theory yielded 18 distinct structures with an energy range of 14.7 kcal/mol. Table 5 compiles the relative energies, predicted chirality, and relevant geometrical parameters of the four lowest energy structures found in the computation. The four lowest energy conformers are shown in Fig. 5. As a general feature we found that the acetic acid has replaced methanol in the hydrogen bond with the quinuclidine amine. In all structures the quinuclidine N is protonated. The methanol is now hydrogen bonded to the acetate.

In the lowest energy conformer **C′** the pro-*R* carbonyl is H-bonded to the catalyst OH so the pro-*S* carbonyl becomes the preferred site for the methoxide nucleophilic attack, in agreement with the observed inversion of enantioselectivity. The corresponding pro-(*R*) conformer **C** is found 2.23 kcal/mol higher in energy, while the next two structures **D** and **D′** featuring pro-*R* and pro-*S* chirality are found 1.10 and 2.17 kcal/mol higher in energy, respectively. Note also the different binding modes in **C** and **D**.

Besides the greater stability of the pro-*R* and pro-*S* conformers in the quinine and quinine–acid catalyzed reactions, respectively, the enantioselectivity is affected by the height of the activation barriers. It is apparent, however, that in order to simulate the interactions within the molecular complexes these need to be treated in their full complexity. Reaction path calculations for such highly fluxional systems are very demanding and they remain beyond the scope of the present study.

The stereochemistry of the product depends on whether methoxide attacks the hydrogen bonded or the non-hydrogen bonded carbonyl. The non-hydrogen bonded carbonyl is in our opinion the site of the methoxide attack. By assuming this we were able to rationalize the observed enantioselectivity in both quinine and quinine–acid catalyzed reactions.

3. Conclusion

A novel room temperature catalytic protocol for enantioselective opening of 3-substituted glutaric *meso*-anhydrides utilizing alkaloid–acid complex was explored in detail.

Its synthetic utility was demonstrated in comparison to the stoichiometric approach at −30 °C in the formal syntheses of sample pharmacological compounds. In both cases good enantioselectivities were found, particularly bearing in mind that glutaric anhydrides typically open with lower enantioselectivities as compared to the succinic.

The option of using a single catalyst, but two protocols to obtain both enantiomers in excess is the most intriguing result, especially as unmodified, easily available, and recyclable catalysts were used.

To rationalize this occurrence, an extensive computational study on the molecular interactions in model compounds was carried out. In all of the low energy structures, the carbonyl oxygen of the anhydride was H-bonded to the hydroxyl group of the catalyst. In

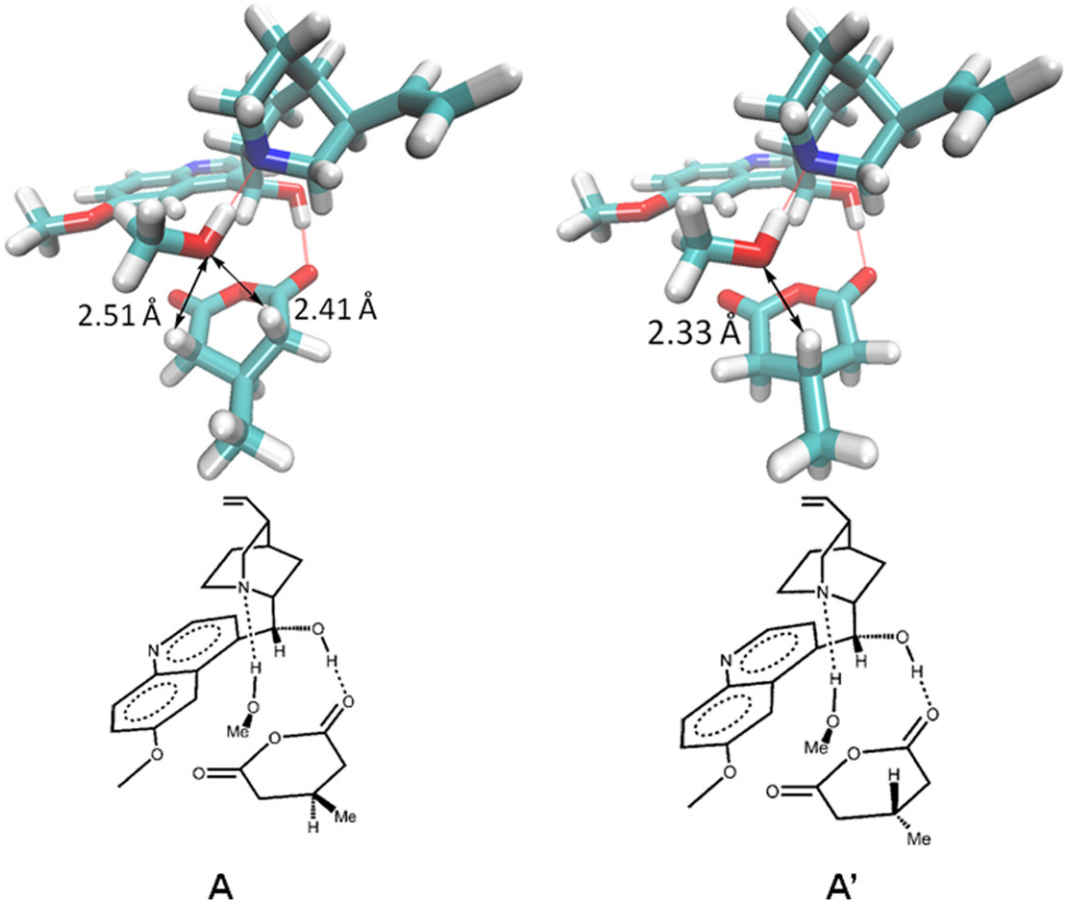

Fig. 4. The structures of the lowest energy conformer (**A**) featuring pro-*R* chirality and the corresponding conformer **A′** leading to the (*S*)-product as obtained with the B3LYP-D3/6-31G(d,p) method. Sterical interactions governing the stability are marked above.

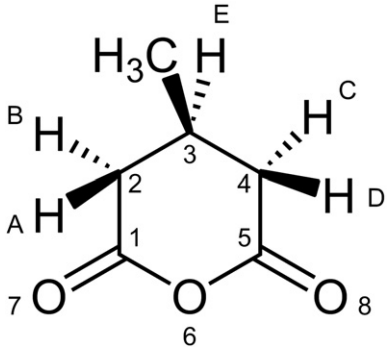

Scheme 3. Numeration of atoms in model anhydride.

Table 5
Relative energies, predicted chirality and relevant geometry parameters of the four lowest energy structures upon addition of acid as computed at the B3LYP/6-31+G(d,p) level

Conf.	*E*/kcal mol^{-1}	Predict. config.	Distance/Å			
			(O,N)[a]	(O,O)[b]	(O,O)[c]	(O,C)[d]
C′	0.00	*S*	2.61	2.83	2.74	3.45
C	2.23	*R*	2.63	2.83	2.71	3.67
D	1.10	*R*	2.58	2.78	2.65	4.98
D′	2.17	*S*	2.58	2.79	2.66	5.19

[a] H-bond distance between acetic acid O–H and quinuclidine N.
[b] H-bond distance between quinine OH and the closest carbonyl O.
[c] H-bond distance between methanol OH and acetate C=O.
[d] Distance between methanol O and anhydride non-hydrogen bonded carbonyl C.

quinine catalyzed reactions the alcohol was directly H-bonded to the quinuclidine nitrogen. Upon acid addition it was found that the acid intercalates between the alcohol and the quinuclidine nitrogen. The net result is that the alcohol approaches the anhydride from the opposite face, in agreement with the observed inversion of enantioselectivity.

4. Experimental section

4.1. Computational details

The calculations were performed using density functional theory (DFT). The conformational landscape of the molecular complexes encompassing quinine, methanol, 3-methylglutaric anhydride, and acetic acid was initially explored at the B3LYP/6-31G(d) level. Several low energy conformers were located. After inverting the stereochemical face of the anhydride, the eight lowest energy structures were reoptimized by using the empirical, dispersion corrected B3LYP-D3 method with the 6-31G(d,p) basis set.[23] The quinine catalyzed opening of *meso*-cyclic anhydrides is governed by medium-strong hydrogen bonding interactions.[24,25] However, we found that the geometries and energetics of the complexes are sensitive to the description of the dispersion interactions. In general, the B3LYP-D3 method yields more compact structures then B3LYP, thus enhancing the energy difference between enantiomers. The calculations were performed by using the Gaussian 03[26] and Turbomole[27] program packages.

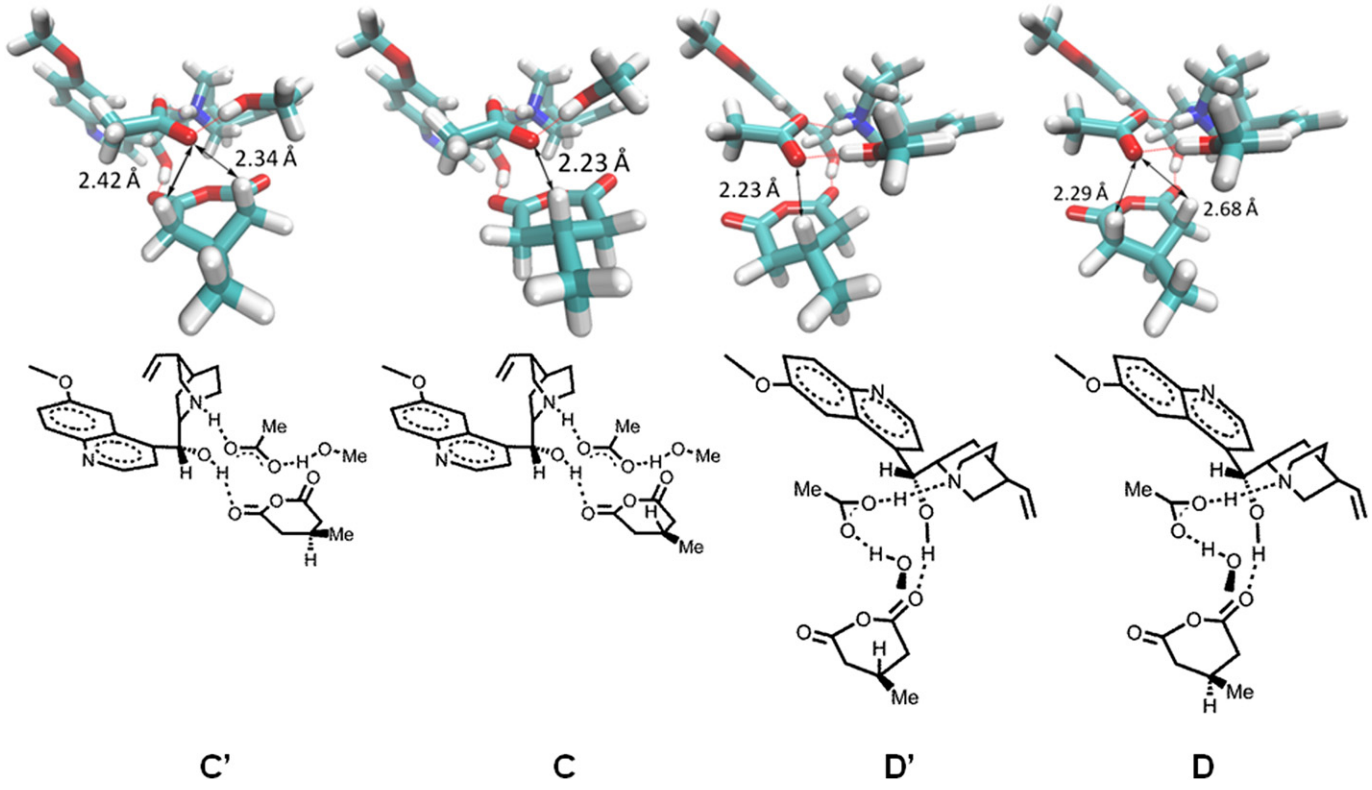

Fig. 5. The structures of the lowest energy conformers of the reaction complexes formed between acetic acid, quinine, methanol, and 3-methylglutaric anhydride. **C**′ and **C** feature pro-*S* and pro-*R* chiralities, respectively, with **C**′ being 2.23 kcal/mol more stable than **C**. The structure of the second most stable conformer (**D**) featuring pro-*R* chirality and the corresponding conformer **D**′ leading to the (*S*)-product is also given. Note that **C**′ is 1.10 kcal/mol more stable than **D**.

4.2. General methods

All reactions were conducted under an argon atmosphere. Anhydride **2** was prepared according to literature.[28]All other reagents and solvents were purchased from commercial sources and used without purification. ^{1}H and ^{13}C NMR were recorded on Bruker AV 300 spectrometer. Chemical shifts (δ_H and δ_C) are quoted in parts per million (ppm), referenced to TMS. High-resolution mass spectrometry (HRMS) was performed on 4800 Plus MALDI TOF/TOF Analyzer. Optical rotations were measured using Optical Activity AA-10 automatic polarimeter. Melting points were determined on Electrothermal 9100 apparatus in open capillaries and are not corrected. For the chemical purity determination, and monitoring of the progress of the reactions Nucleosil 100-5 C18 column was used (50% methanol in water with 0.5% H_3PO_4 to 100% methanol). ees of monoesters **4** and **6** were determined on Chiralpak AS column (hexane/EtOH/TFA=98:2:0.1) and Chiralpak OD column (hexane/EtOH/TFA=95:5:0.1), respectively.

4.3. Method A

To the 0.1 M toluene solution of anhydride (10 mmol), alkaloid (0.1 equiv), xanthene-9-carboxylic acid (0.2 equiv), and alcohol (1.5 equiv) were added. The reaction mixture was stirred until >90% conversion was reached (see Table 3) and the reaction was stopped by the addition of 5% HCl. The organic layer was washed once more with 5% HCl and evaporated. The oily residue was dissolved in 2% K_2CO_3 and washed successively with EtOAc. The aqueous solution was then carefully acidified with H_3PO_4 to pH 5.4 and extracted with toluene. The organic extracts were dried over Na_2SO_4 and evaporated in vacuo.

4.4. Method B

To the cold 0.1 M toluene solution of anhydride (10 mmol), alkaloid (1.1 equiv) and alcohol (1.5 equiv) were added. The reaction mixture was stirred until >90% conversion was reached (see Table 3) and the reaction was stopped by the addition of 5% HCl. The organic layer was washed once more with 5% HCl and evaporated. Oily residue was dissolved in 2% K_2CO_3 and washed successively with EtOAc. Aqueous solution was acidified with HCl to pH 2 and extracted with EtOAc. The organic extracts were dried over Na_2SO_4 and evaporated in vacuo.

4.5. Compounds characterization

*4.5.1. (R)-3-Isobutyl-pentanedioic acid monobenzyl ester (**4**).* Yellowish oil; $[\alpha]_D^{26}$ −1.9 (*c* 3.166, EtOH) for 73% ee; ν_{max} (KBr)= 3600–2800 (br), 3035, 2960, 2870, 1738, 1707, 1456, 1388, 1236, 1163, 753, 698 cm^{-1}; ^{1}H NMR (300 MHz, $CDCl_3$, 25 °C, TMS): δ=9.88 (br s, 1H), 7.28–7.42 (m, 5H), 5.08–5.14 (s, 2H), 2.35–2.45 (m, 5H), 1.52–1.68 (m, 1H), 1.16–1.24 (m, 2H), 0.82–0.92 (dd, 6H, J_1=6.7 Hz, J_2=3.2 Hz) ppm; ^{13}C NMR (75 MHz, $CDCl_3$, 25 °C, TMS): δ=178.6, 172.4, 135.9, 128.6, 128.3, 128.2, 66.3, 43.3, 38.6, 38.4, 29.8, 25.2, 22.5, 22.5 ppm; HRMS (MALDI): MK^+, found 317.1145. $C_{16}H_{22}O_4$ requires 317.1149.

*4.5.2. (R)-3-(4-Chloro-phenyl)-pentanedioic acid monobenzyl ester (**6**).* White powder; mp 143.2–144.8 °C; $[\alpha]_D^{25}$ −4.6 (*c* 1.192, EtOH) for 77% ee; ν_{max} (KBr)=3600–2800 (br), 2940, 1733, 1719, 1675, 1493, 1415, 1232, 1152, 825, 733, 692 cm^{-1}; ^{1}H NMR (300 MHz, $CDCl_3$, 25 °C, TMS): δ=10.60 (br s, 1H), 7.08–7.39 (m, 9H), 4.95–5.12 (s, 2H), 3.55–3.70 (m, 1H), 2.55–2.85 (m, 4H) ppm; ^{13}C NMR (75 MHz, $CDCl_3$, 25 °C, TMS): δ=177.0, 171.1, 140.5, 135.5, 132.9,

128.8, 128.7, 128.5, 128.3, 128.3, 66.5, 40.5, 40.0, 37.5 ppm; HRMS (MALDI): MNa^+ found 355.0707. $C_{18}H_{17}O_4Cl$ requires 355.0707.

Acknowledgements

We thank the Ministry of Science, Education and Sports of the Republic of Croatia for financing (grant nos. 098-0982933-2908 and 098-0352851-2921).

Supplementary data

Supplementary data associated with this article can be found in the online version, at http://dx.doi.org/10.1016/j.tet.2012.07.035. These data include MOL files and InChiKeys of the most important compounds described in this article.

References and notes

1. (a) Rodriguez-Docampo, Z.; Connon, S. J. *ChemCatChem* **2012**, *4*, 151–168; (b) Atodiresei, I.; Schiffers, I.; Bolm, C. *Chem. Rev.* **2007**, *107*, 5683–5712; (c) Chen, Y.; McDaid, P.; Deng, L. *Chem. Rev.* **2003**, *103*, 2965–2984.
2. Starr, J. T.; Koch, G.; Carreira, E. M. *J. Am. Chem. Soc.* **2000**, *122*, 8793–8794.
3. Tanyeli, C.; Özçubukçu, S. *Tetrahedron: Asymmetry* **2003**, *14*, 1167–1170.
4. Mittendorf, J.; Benet-Buchholz, J.; Fey, P.; Mohrs, K. H. *Synthesis* **2003**, *1*, 136–140.
5. Keen, S. P.; Cowden, C. J.; Bishop, B. C.; Brands, K. M. J.; Davies, A. J.; Dolling, U. H.; Lieberman, D. R.; Stewart, G. W. *J. Org. Chem.* **2005**, *70*, 1771–1779.
6. (a) Hameršak, Z.; Stipetić, I.; Avdagić, A. *Tetrahedron: Asymmetry* **2007**, *18*, 1481–1485; (b) Peschiulli, A.; Procuranti, B.; O'Connor, C. J.; Connon, S. J. *Nat. Chem.* **2010**, *2*, 380–384.
7. Huang, J.; Xiong, F.; Chen, F. E. *Tetrahedron: Asymmetry* **2008**, *19*, 1436–1443.
8. Ji, L.; Ma, Y.; Li, J.; Zhang, L.; Zhang, L. *Tetrahedron Lett.* **2009**, *50*, 6166–6168.
9. Hiratake, J.; Inagaki, M.; Yamamoto, Y.; Oda, J. *J. Chem. Soc., Perkin Trans. 1* **1987**, 1053–1058.
10. Aitken, R. A.; Gopal, J.; Hirst, J. A. *J. Chem. Soc., Chem. Commun.* **1988**, 632–634.
11. Bolm, C.; Schiffers, I.; Atodiresei, I.; Hackenberger, C. P. R. *Tetrahedron Asymmetry* **2003**, *14*, 3455–3467.
12. Chen, Y.; Tian, S.-K.; Deng, L. *J. Am. Chem. Soc.* **2000**, *122*, 9542–9543.
13. Peschiulli, A.; Gun'k, Y.; Connon, S. J. *J. Org. Chem.* **2008**, *73*, 2454–2457.
14. Park, S. E.; Nam, E. H.; Jang, H. B.; Oh, J. S.; Some, S.; Lee, Y. S.; Song, C. E. *Adv. Synth. Catal.* **2010**, *352*, 2211–2217.
15. Ivšić, T.; Hameršak, Z. *Tetrahedron: Asymmetry* **2009**, *20*, 1095–1098.
16. Bigi, F.; Carloni, S.; Maggi, R.; Mazzacani, A.; Sartori, G.; Tanzi, G. *J. Mol. Catal., A: Chem.* **2002**, *182*, 533–539.
17. Dedeoglu, B.; Catak, S.; Houk, K. N.; Aviyente, V. *ChemCatChem* **2010**, *2*, 1122–1129.
18. Schmitt, E.; Schiffers, I.; Bolm, C. *Tetrahedron* **2010**, *66*, 6349–6357.
19. Oh, S. H.; Rho, H. S.; Lee, J. W.; Lee, J. E.; Youk, S. H.; Chin, J.; Song, C. E. *Angew. Chem., Int. Ed.* **2008**, *47*, 7872–7875.
20. Rho, H. S.; Oh, S. H.; Lee, J. W.; Lee, J. Y.; Chin, J.; Song, C. E. *Chem. Commun.* **2008**, 1208–1210.
21. Caner, H.; Biedermann, P. U.; Agranat, I. *Chirality* **2003**, *15*, 637–645.
22. (a) Bürgi, T.; Baiker, A. *J. Am. Chem. Soc.* **1998**, *120*, 12920–12926; (b) Meier, D. M.; Urakawa, A.; Turrà, N.; Rüegger, H.; Baiker, A. *J. Phys. Chem. A* **2008**, *112*, 6150–6158; (c) Urakawa, A.; Meier, D. M.; Rüegger, H.; Baiker, A. *J. Phys. Chem. A* **2008**, *112*, 7250–7255; (d) Balzano, F.; Jumde, R. P.; Mandoli, A.; Masi, S.; Pini, D.; Uccello-Barretta, G. *Chirality* **2011**, *23*, 784–795.
23. (a) Grimme, S.; Antony, J.; Ehrlich, S.; Krieg, H. *J. Chem. Phys.* **2010**, *132*, 154104–154123; (b) Grimme, S.; Ehrlich, S.; Goerigk, L. *J. Comput. Chem.* **2011**, *32*, 1456–1465; (c) Hujo, W.; Grimme, S. *Phys. Chem. Chem. Phys.* **2011**, *13*, 13942–13950.
24. (a) Hadži, D. *Theoretical Treatments of Hydrogen Bonding*; John Wiley Sons: Chichester, UK, New York, NY, 1997; (b) Giese, K.; Petković, M.; Naundorf, H.; Kühn, O. *Phys. Rep.* **2006**, *430*, 211–276.
25. (a) Matanović, I.; Došlić, N.; Mihalić, Z. *Chem. Phys.* **2004**, *306*, 201–207; (b) Petković, M.; Novak, J.; Došlić, N. *Chem. Phys. Lett.* **2009**, *474*, 248–252.
26. Frisch, M. J.; Trucks, G. W.; Schlegel, H. B.; Scuseria, G. E.; Robb, M. A.; Cheeseman, J. R.; Montgomery, J. A., Jr.; Vreven, T.; Kudin, K. N.; Burant, J. C.; Millam, J. M.; Iyengar, S. S.; Tomasi, J.; Barone, V.; Mennucci, B.; Cossi, M.; Scalmani, G.; Rega, N.; Petersson, G. A.; Nakatsuji, H.; Hada, M.; Ehara, M.; Toyota, K.; Fukuda, R.; Hasegawa, J.; Ishida, M.; Nakajima, T.; Honda, Y.; Kitao, O.; Nakai, H.; Klene, M.; Li, X.; Knox, J. E.; Hratchian, H. P.; Cross, J. B.; Bakken, V.; Adamo, C.; Jaramillo, J.; Gomperts, R.; Stratmann, R. E.; Yazyev, O.; Austin, A. J.; Cammi, R.; Pomelli, C.; Ochterski, J. W.; Ayala, P. Y.; Morokuma, K.; Voth, G. A.; Salvador, P.; Dannenberg, J. J.; Zakrzewski, V. G.; Dapprich, S.; Daniels, A. D.; Strain, M. C.; Farkas, O.; Malick, D. K.; Rabuck, A. D.; Raghavachari, K.; Foresman, J. B.; Ortiz, J. V.; Cui, Q.; Baboul, A. G.; Clifford, S.; Cioslowski, J.; Stefanov, B. B.; Liu, G.; Liashenko, A.; Piskorz, P.; Komaromi, I.; Martin, R. L.; Fox, D. J.; Keith, T.; Al-Laham, M. A.; Peng, C. Y.; Nanayakkara, A.; Challacombe, M.; Gill, P. M. W.; Johnson, B.; Chen, W.; Wong, M. W.; Gonzalez, C.; Pople, J. A. *Gaussian 03, Revision E.01*; Gaussian, Inc.: Pittsburg PA, 2003.
27. Ahlrichs, R.; Bär, M.; Häser, M.; Horn, H.; Kölmel, C. *Chem. Phys. Lett.* **1989**, *162*, 165–169.
28. Smith, W. T.; Kort, P. G. *J. Am. Chem. Soc.* **1950**, *72*, 1877–1878.